ChemPubSoc Europe

DOI: 10.1002/chem.201304443

CHEMISTRY
A European Journal
Full Paper

Surface Reactivity

# A Single-Molecule-Level Mechanistic Study of Pd-Catalyzed and Cu-Catalyzed Homocoupling of Aryl Bromide on an Au(111) Surface

Jinne Adisoejoso,[a] Tao Lin,[a] Xue Song Shang,[b] Ke Ji Shi,[b] Aditi Gupta,[a] Pei Nian Liu,*[b] and Nian Lin*[a]

**Abstract:** On-surface Pd- and Cu-catalyzed C–C coupling reactions between phenyl bromide functionalized porphyrin derivatives on an Au(111) surface have been investigated under ultra-high vacuum conditions by using scanning tunneling microscopy and kinetic Monte Carlo simulations. We monitored the isothermal reaction kinetics by allowing the reaction to proceed at different temperatures. We discovered that the reactions catalyzed by Pd or Cu can be described as a two-phase process that involves an initial activation followed by C–C bond formation. However, the distinctive reaction kinetics and the C–C bond-formation yield associated with the two catalysts account for the different reaction mechanisms: the initial activation phase is the rate-limiting step for the Cu-catalyzed reaction at all temperatures tested, whereas the later phase of C–C formation is the rate-limiting step for the Pd-catalyzed reaction at high temperature. Analysis of rate constants of the Pd-catalyzed reactions allowed us to determine its activation energy as $(0.41 \pm 0.03)$ eV.

## Introduction

Covalent coupling on surfaces provides an alternative strategy to traditional wet chemistry, and during the last few years a variety of such on-surface reactions have been reported.[1–25] By confining reactive species to a surface, it may become possible to execute reactions and synthesize structures that are not accessible in solution. The first and one of the most extensively studied reactions is Ullmann coupling between haloarenes. This reaction has been applied successfully in the past to engineer one- and two-dimensional covalent architectures under ultra-high vacuum (UHV) conditions.[4,5,12,15,16,20,24,25] Although a large variety of on-surface reactions has been explored, the experimental analysis of the reaction mechanism including the determination of rate constants and activation energies still remains a great challenge because the myriad techniques developed for reactions in solution do not apply. Herein, we report an investigation for uncovering the reaction mechanism of C–C bond formation between molecules of 5,15-bis-(4-bromophenyl)-10,20-diphenyl porphyrin (**1**; Figure 1a) by using Pd or Cu as catalysts. Pd is the most versatile catalyst used in homocoupling and cross-coupling reactions in solution, and hundreds of organic reactions that involve various covalent bond formation have been successfully achieved.[26,27] Exploring Pd-catalyzed on-surface reactions is therefore very appealing. We determined reaction yields, rate constants, and activation

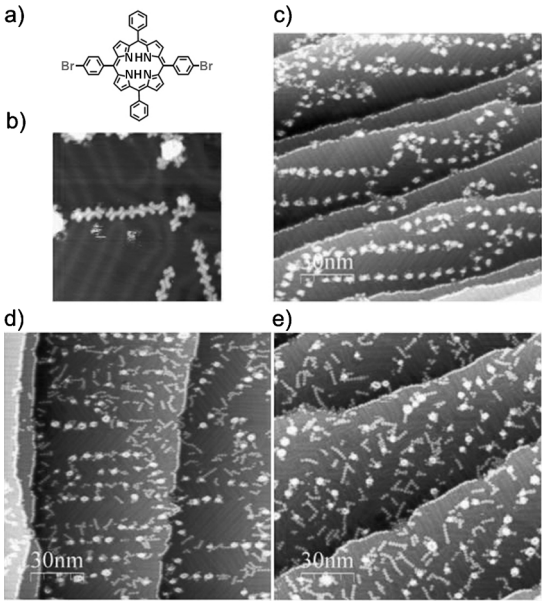


**Figure 1.** a) Chemical structure of **1**. b) STM image ($25 \times 25$ nm$^2$) showing polymeric chains formed by **1** in the presence of Pd. c–e) Representative STM images of Pd-catalyzed polymerization of **1** with annealing at 447 K for c) 5, d) 45, and e) 105 min.

[a] *Dr. J. Adisoejoso, T. Lin, A. Gupta, Prof. Dr. N. Lin*
*Department of Physics*
*The Hong Kong University of Science and Technology*
*Clear Water Bay, Hong Kong (P.R. China)*
*E-mail: phnlin@ust.hk*

[b] *X. S. Shang, K. J. Shi, Prof. Dr. P. N. Liu*
*Shanghai Key Laboratory of Functional Materials Chemistry*
*and Institute of Fine Chemicals*
*East China University of Science and Technology,*
*Meilong Road 130, Shanghai (P.R. China)*
*E-mail: liupn@ecust.edu.cn*

energy by monitoring isothermal reaction products in situ using scanning tunneling microscopy (STM) at single-molecule resolution.[28] Moreover, we simulated the reactions using kinetic Monte Carlo simulations to understand the reaction mechanism. Our findings revealed a two-phase process that involves an initial activation followed by C–C bond formation for both catalysts. The comparison between the bond-formation yields and the reaction kinetics, however, indicated that the two catalysts lower the reaction barrier differently so that the rate-limiting step in the Cu-catalyzed processes is the initial activation phase, whereas in the Pd-catalyzed processes the rate-limiting step is the later phase of C–C formation.

## Results and Discussion

In a previous study, we showed that **1** undergoes Cu-catalyzed Ullmann coupling on an Au(111) surface at 453 K and forms covalently linked polymeric chains.[29] We observed similar polymeric chains when the same reaction was carried out in the presence of Pd catalyst. Figure 1b shows that adjacent monomers in a polymeric chain are spaced with a center-to-center distance of $(1.74 \pm 0.04)$ nm, which is consistent with the distance between covalently linked porphyrin molecules.[15,29] Note that in the absence of Pd or Cu, annealing similar molecules on clean Au(111) up to approximately 453 K for 30 min only yielded 1.5% covalently linked species.[29] Therefore the polymeric chains formed at low temperature in the presence of Pd or Cu can be attributed to a homocoupling reaction catalyzed by Cu or Pd.[24,25]

We examined the reaction kinetics of C–C bond formation between monomers of **1** in the presence of Pd. First we deposited **1** on the Au(111) surface, which was precovered by Pd, held at room temperature, and then the sample was annealed in 10–12 steps and 8–10 min for each step. After each annealing step, the sample was cooled to room temperature and measured by STM.[28] The same procedure was conducted at five annealing temperatures (393, 411, 429, 447, and 465 K, all $\pm 2$ K). STM images acquired at different surface locations were analyzed, covering a total area of about $2 \times 10^5$ nm$^2$. Dimers and longer chains were clearly visible in the STM images, which allowed us to determine the number of bonds formed as a function of reaction time and temperature. Monomers, however, were not distinguishable in the images because they were highly dynamic at room temperature; as a result, molecular concentration appeared lower at shorter reaction times. The STM images clearly show an increase in the number of polymeric chains with longer reaction time (Figure 1c–e). The time-dependent increase in C–C bond concentration was observed at all annealing temperatures tested (Figure 2a). At 429, 447, and 465 K, bond concentration initially rises rapidly; after 20 min, the rising trend slows down, and the bond concentration gradually reaches saturation. As expected, the initial increase in the bond concentration is more rapid at higher temperatures. At 411 K, however, the initial rapid increase is not as apparent as those observed at the higher temperatures. At 393 K, a two-phase behavior appears (Figure 2b): a relatively slow increase (0–60 min, defined as phase I) is followed by a rapid increase (60–140 min, defined as phase II). The two-phase character suggests that the coupling reaction involves multiple steps. In solution, Pd-catalyzed homocoupling of aryl halides is known to involve multiple steps: oxidative addition, which forms an intermediate organopalladium complex; then transmetalation; and finally reductive elimination, which regenerates the Pd catalyst.[26] We speculate that the on-surface reaction might follow a similar mechanism, though the details may differ. We propose that phase I can be associated with an initial activation process, whereas phase II involves C–C bond formation.

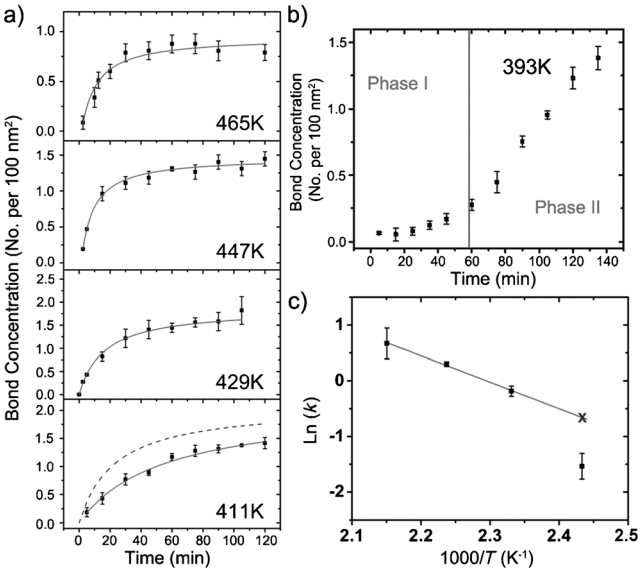


**Figure 2.** a) Bond concentration in Pd-catalyzed homocoupling of **1** on Au(111) as a function of reaction time at 411, 429, 447, and 465 K. Solid curves were fitted using Equation (2). b) Bond concentration as a function of annealing time at 393 K showing a two-phase behavior. c) Arrhenius plot of rate constant $k$ obtained from the data in (a).

We could not analyze phase I or its kinetics because of high monomer mobility. Nevertheless, our data showed that phase I occurred faster than phase II at high temperature because it became undetectable above 411 K (Figure 2a). Therefore, the rate-limiting step at higher temperatures appears to be C–C bond formation, which allowed us to calculate the activation energy from reaction kinetics. The overall reaction can be represented as follows.

If we define [bond] as the concentration of the C–C bonds formed and [phenyl-Br] as the concentration of the unreacted phenyl bromide, the rate equation can be written as [Eq. (1)]:

$$d[\text{bond}]/dt = k[\text{phenyl-Br}]^2 \quad (1)$$

The bond concentration can be derived from Equation (1) as [Eq. (2)]:

$$[\text{bond}] = \frac{kt[\text{phenyl} - \text{Br}]_0^2}{1 + 2kt[\text{phenyl} - \text{Br}]_0} + [\text{bond}]_0 \quad (2)$$

in which [phenyl-Br]$_0$ refers to the initial concentration of the phenyl bromide, and [bond]$_0$ refers to the bond concentration prior to annealing. Presumably these bonds were formed during the evaporation of **1**.

Table 1 lists the fitting parameters for the four sets of kinetic data shown in Figure 2a using Equation (2). The rate constant $k$ depends on temperature $T$ according to the Arrhenius equation. The plot of ln($k$) versus $T^{-1}$ shows a linear relationship for

**Table 1.** Fitting parameters for the kinetic data shown in Figure 2a using Equation (2).

| Annealing temperature [K] | Rate constant ($k\times100$) [$s^{-1}nm^{-2}$] | [phenyl-Br]$_0$ [No. per 100 nm$^2$] | [bond]$_0$ [No. per 100 nm$^2$] |
|---|---|---|---|
| 411 | $0.215\pm0.056$ | $4.2\pm0.002$ | $0.59\pm0.02$ |
| 429 | $0.831\pm0.080$ | $3.7\pm0.002$ | $0.90\pm0.03$ |
| 447 | $2.184\pm0.090$ | $3.5\pm0.001$ | $0.038\pm0.002$ |
| 465 | $2.747\pm0.877$ | $2.3\pm0.002$ | $0.17\pm0.02$ |

the three reaction temperatures above 420 K (Figure 2c), but not for 411 K. We interpret this behavior as follows. Above 420 K, phase I does not limit the overall reaction rate, so the rate can be modeled by using Equation (1). Below 420 K, however, phase I cannot be neglected, so Equation (2) cannot accurately describe the reaction rate. If we neglect phase I at 411 K, a higher rate constant is expected, as marked by an "×" in Figure 2c. This hypothesized rate constant corresponds to a bond concentration profile represented by the dashed curve in the bottom panel of Figure 2a. The actual bond concentration is below this hypothesized profile, which indicates that phase I indeed limits the overall reaction at this temperature. The linear fit for the three high-temperature reaction rate constants gives an activation energy of $(0.41\pm0.03)$ eV and a prefactor of $(3\times10^{6\pm1})$ $s^{-1}nm^{-2}$ for the overall reaction. Although we were unable to determine the activation energy for each phase separately, the much faster kinetics of phase I imply that its activation energy is lower, thus the obtained activation energy is close to that of phase II alone, that is, C–C bond formation. This value is much lower than the activation energy of 1.12 eV reported for the Ullmann coupling of iodobenzene on Cu(111).[30] Given that Br is less reactive than I, we conclude that Pd lowers the reaction barrier much more efficiently than Cu does.

To compare the performance of Pd and Cu as catalysts under the same conditions, we repeated our experiments using Cu as catalyst. At four temperatures (399, 417, 435, and 453 K, all $\pm2$ K), the bond concentration increases slowly initially up to 90 min, then increases faster from 90 min onwards (Figure 3a); this is somehow similar to the trend observed for Pd at 393 K (Figure 2b). Figure 3b–d shows representative STM images of the sample annealed at 453 K for different duration. Clearly, these data exhibit very different characteristics than the Pd-catalyzed samples (see Figure 1). We will discuss the differences in detail later. Here we would like to emphasize that on-surface Cu-mediated C–C coupling was also suggested to

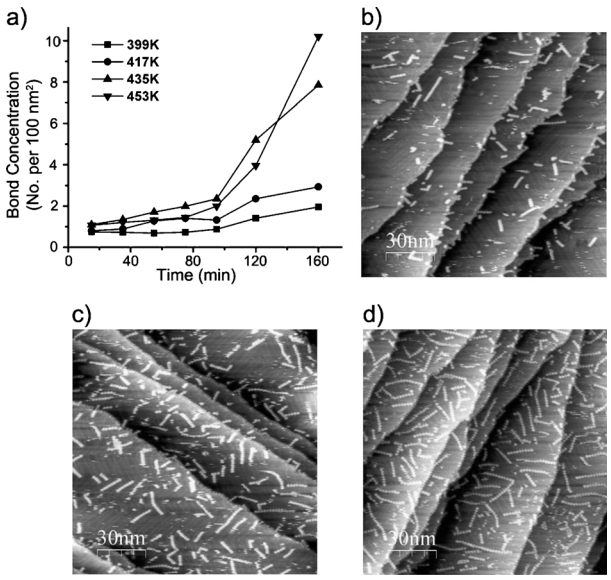


**Figure 3.** a) Bond concentration in Cu-catalyzed homocoupling of **1** on Au(111) as a function of reaction time at 399 (■), 417 (●), 435 (▲), and 453 K (▼, the 453 K data are scaled down by a factor of five). b–d) Representative STM image of the Cu-catalyzed reaction after annealing at 453 K for b) 5, c) 75, and d) 160 min.

occur in multiple steps: monomer deposition, cleavage of weakly bound halogen atoms to generate surface-stabilized radicals, and coupling of these radicals in addition reactions.[20,31,32] We could not identify which of these steps is rate-limiting under our experimental conditions, which prevented us from calculating the activation energy using simple reaction kinetics. Nevertheless, on the basis of the clear presence of the initial slow phase at all annealing temperatures tested, we suggest that the initial activation step in the Cu-catalyzed reaction has a higher activation energy than phase I in the Pd-catalyzed process.

We have found that the two catalysts resulted in sharply different C–C bond formation yield and length distribution of the polymeric chains. In our experiments, the initial molecule dosage was kept constant, and the catalysts were used in excess amounts with respect to the molecules. Figure 2a and Table 1 show that the yield of the Pd-catalyzed reaction does not increase at higher reaction temperatures but declines slightly. In contrast, Figure 3a reveals that the yield of the Cu-catalyzed reactions increases significantly at higher temperatures, an approximately 25-fold increase from 393 to 453 K. Furthermore, the yields of the Pd-catalyzed reaction are much lower than those of the Cu-catalyzed ones, for example, two bonds per 100 nm$^2$ versus 50 bonds per 100 nm$^2$ formed at the longest annealing tested in the experiments. In addition to the different yields, Figure 3d clearly reveals that the Cu-catalyzed reactions generated longer polymeric chains than those formed in the Pd-catalyzed reactions, as seen in Figure 1d. Figure 4 displays the length distributions of the polymers formed by Pd-catalyzed (Figure 4a–d) and Cu-catalyzed (Figure 4e–h) reactions at different temperatures and different reaction durations. One can see that Pd-catalyzed reactions re-

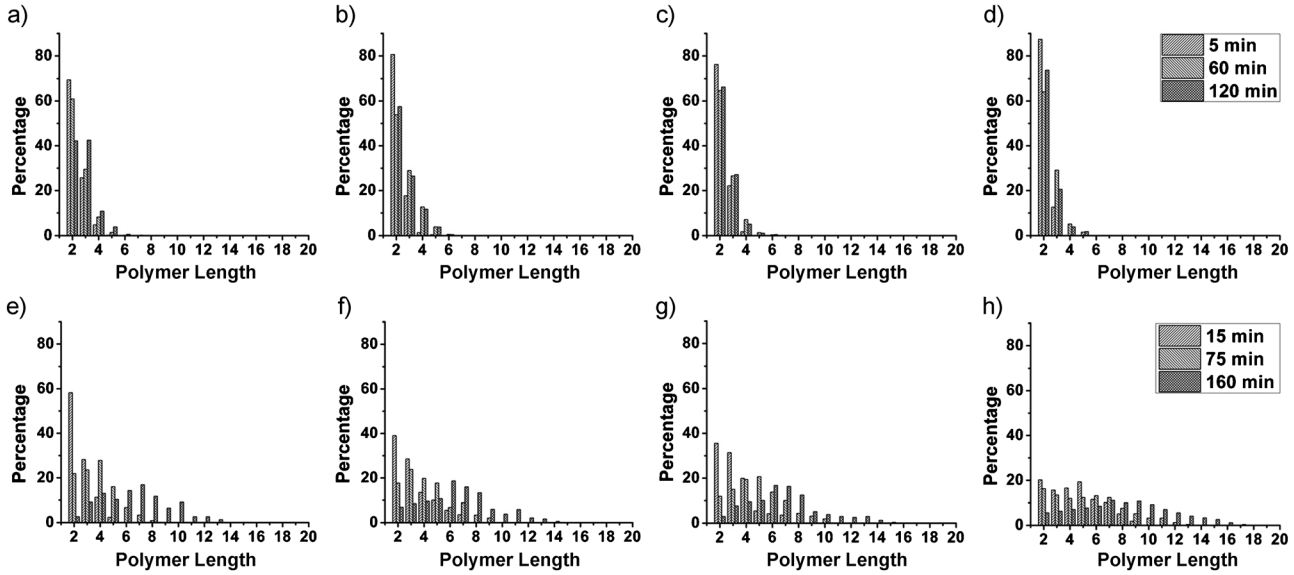


**Figure 4.** Length distribution of the polymers formed in the presence of Pd for annealing at a) 411, b) 429, c) 447, d) and 465 K; and in the presence of Cu for annealing at e) 399, f) 417, g) 435, and h) 453 K. Polymer length refers to the number of monomers in a chain.

sulted in a narrow distribution from dimers to hexamers, with dimers predominating, regardless of the annealing conditions. In contrast, longer Cu-catalyzed reactions formed much broader polymer-length distribution with no apparent length preference; the longest observed polymer consisted of 17 monomers.

These contrasts suggest that the two catalysts lower the reaction barrier in different ways. In an attempt to understand the apparent different behavior between Pd and Cu catalysts, we simulated the coupling reaction using a kinetic Monte Carlo (KMC) algorithm.[29,33] The reaction was simulated as a two-step process: 1) the phenyl bromide end of a monomer is activated with an energy barrier of $E_1$; 2) when an activated end of one monomer encounters an unactivated end of another monomer, a C–C bond is formed with an energy barrier of $E_2$.[26] Both steps are non-reversible. We set $E_1$ to be larger for Cu ($E_1 = 0.50$ eV) than for Pd ($E_1 = 0.35$ eV) on the basis of our observation that phase I was undetectable in the Pd-catalyzed reaction at temperatures above 410 K, whereas it was observable in the Cu-catalyzed reaction at temperatures up to 453 K. The value of $E_2$ was set at 0.40 eV for both processes. The simulation results of the two sets of parameters are shown in Figure 5a and b, in which one can see that the lower $E_1$ leads to shorter chains, whereas the higher $E_1$ leads to longer chains. The simulated polymer-length distributions are plotted in Figure 5c, which displays a narrow distribution with dimers as the predominant product given by the lower $E_1$, and a broader distribution towards longer chains given by the higher value of $E_1$. The yields of the C–C bond formed in the two processes are 10.5 and 67.7%, respectively, thus indicating that the lower $E_1$ results in a lower yield. The simulations provide some hints as to why Pd-catalyzed reactions give rise to low yields and shorter polymeric length: the first-phase reaction is very efficient, so the population of the unactivated species is reduced rapidly. As a result, the activated species have less of a chance

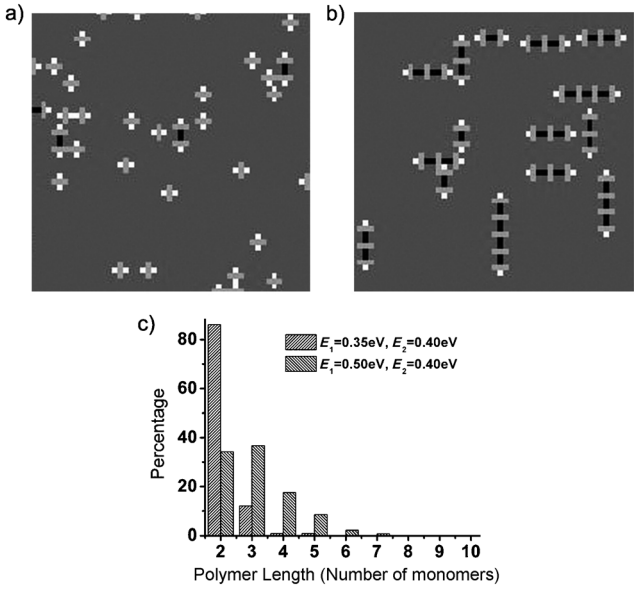


**Figure 5.** KMC-simulated polymeric chains after 120 min at 400 K of a) $E_1 = 0.35$ eV, $E_2 = 0.40$ eV and b) $E_1 = 0.50$ eV, $E_2 = 0.40$ eV. White tips represent the activated ends, and black bars represent the C–C bonds. c) Polymer-length distributions obtained from the simulations.

to encounter unactivated monomers, hence C–C formation is suppressed and growth into longer chains is unfavorable. Although the simulations do not reproduce the experimental results quantitatively, they do suggest that lower $E_1$ in a two-step reaction leads to shorter chains and lower yield.

## Conclusion

Pd and Cu were successfully applied as catalysts in the homocoupling of aryl-bromide-functionalized porphyrin molecules on an Au(111) surface. By means of analyzing the isothermic re-

action series and determining the bond concentration as a function of reaction temperature and duration, we discovered that the reactions involve multiple steps for Cu and Pd catalysts. However, the two catalysts result in distinctive bond formation yields as well as reaction rates. These differences are attributed to mechanistic differences between the roles the two catalysts play in the reaction. The activation energy of Pd catalysis was measured to be $(0.41 \pm 0.03)$ eV, which is much lower than the Cu catalysis.

## Experimental Section

The synthesis of **1** has been discussed earlier.[29] Experiments were performed in an ultra-high vacuum system (Omicron Nanotechnology) with a base pressure below $5 \times 10^{-10}$ mbar. A single crystalline Au(111) substrate was prepared by argon-ion sputtering and annealing at approximately 630 °C. Pd atoms were deposited by heating a W filament wrapped with a Pd wire using a 3.5 A current. The dosage of the deposited Pd on the surface is 0.5–0.6 atoms $nm^{-2}$. Cu atoms were deposited using an electron-beam evaporator, and the dosage on the surface was 1.0–1.1 atoms $nm^{-2}$. The crucible that contained the molecule was heated in an organic molecular beam deposition source (Dodecon) to the evaporation temperature (320 °C), and the molecules were deposited on the surface held at room temperature. The molecule dosage was kept at a constant in the experiments. The molecule-to-metal ratio was approximately 1:5 for the Pd and approximately 1:10 for the Cu. STM characterization was performed at room temperature in a constant current mode at 1.0–1.5 V positive or negative bias and at 0.2–0.3 nA tunneling current. Bond-concentration values and length-distribution graphs were obtained by counting the number of covalently linked monomers from STM images of a total area of approximately $2 \times 10^5$ $nm^2$. To achieve a better temperature and duration control for the annealing steps, the samples were introduced into a heating stage, which was already heated to the desired temperature, and then they were moved from the heating stage to the sample stage when the desired time duration was reached. The sample stage was held at room temperature. The heat capacitance of the sample was much smaller than that of the heating stage, as we never observed any temperature fluctuation when the sample was introduced into the heating stage. For each annealing temperature, one single sample was used, which was annealed and measured in subsequent cycles. The fate of the Br atoms after the reaction cannot be identified on the basis of the experimental data. Nevertheless, given that the morphology of the Pd/Cu islands remains unchanged throughout the annealing period, one can rule out that the split-off Br atoms interfere with the Pd/Cu catalyst.

The kinetic Monte Carlo (KMC) simulations were performed on a $200 \times 200$ square lattice, which amounts to one monolayer of molecules that contained $66 \times 66$ monomers. Periodic boundary conditions were applied. Initially, 400 monomers were deposited randomly onto the substrate lattice. Desorption of the monomers from the substrate was not allowed. The monomers can hop to the nearest-neighboring unoccupied sites or rotate by 90° clockwise or counterclockwise. The energy barriers of hopping and rotation are 0.68 and 1.00 eV, respectively. Each monomer contained two Br ends at *trans* positions. The rates of each event are given by $r = v \times \exp(-E/kT)$, in which $v$ is the attempting frequency and $k$ is the Boltzmann constant. The attempting frequency was set as $1 \times 10^{12}$ Hz for monomer jumping and rotation and $1 \times 10^7$ Hz for C–C bond formation in the second step. In step 1, since the reaction occurs when an activated end of the monomers encounters a catalyst atom, we used a smaller frequency ($v = 1 \times 10^5$ Hz) to account for the reduced probability that arises from finite Pd or Cu concentration. The details of the KMC simulation algorithm can be found in the literature.[33]

## Acknowledgements

This work was supported financially by the Hong Kong Research Grants Council (project no. 602712), the National Natural Science Foundation of China (project nos. 21172069 and 21190033), the Innovation Program of Shanghai Municipal Education Commission (project no. 12ZZ050), and the Fundamental Research Funds for the Central Universities.

**Keywords:** copper · kinetics · palladium · scanning probe microscopy · surface chemistry

[1] M. Lackinger, W. M. Heckl, *J. Phys. D* **2011**, *44*, 464011.
[2] J. A. A. W. Elemans, S. Lei, S. De Feyter, *Angew. Chem.* **2008**, *120*, 7434–7469; *Angew. Chem. Int. Ed.* **2008**, *48*, 7298–7332.
[3] N. A. A. Zwaneveld, R. Pawlak, M. Abel, D. Catalin, D. Gigmes, D. Bertin, L. Porte, *J. Am. Chem. Soc.* **2008**, *130*, 6678–6679.
[4] M. Bieri, M. Treier, J. Cai, K. Aït-Mansour, P. Ruffieux, O. Gröning, P. Gröning, M. Kastler, R. Rieger, X. Feng, K. Müllen, R. Fasel, *Chem. Commun.* **2009**, 6919–6921.
[5] R. Gutzler, H. Walch, G. Eder, S. Kloft, W. M. Heckl, M. Lackinger, *Chem. Commun.* **2009**, 4456–4458.
[6] M. Abel, S. Clair, O. Ourdjini, M. Mossoyan, L. Porte, *J. Am. Chem. Soc.* **2011**, *133*, 1203–1205.
[7] H.-Y. Gao, H. Wagner, D, Zhong, J.-H. Franke, A. Studer, H. Fuchs, *Angew. Chem.* **2013**, *125*, 4116–4120; *Angew. Chem. Int. Ed.* **2013**, *52*, 4024–4028.
[8] M. In't Veld, P. Iavicoli, S. Haq, D. B. Amabilino, R. Raval, *Chem. Commun.* **2008**, 1536–1538.
[9] Y.-Q. Zhang, N. Kepčija, M. Kleinschrodt, K. Diller, S. Fischer, A. C. Papageorgiou, F. Allegretti, J. Björk, S. Klyatskaya, F. Klappenberger, M. Ruben, J. V. Barth, *Nat. Commun.* **2012**, *3*, 1286.
[10] D. Zhong, J.-H. Franke, S. K. Podiyanachari, T. Blömker, H. Zhang, G. Kehr, G. Erker, H. Fuchs, L. Chi, *Science* **2011**, *334*, 213–216.
[11] J. A. Lipton-Duffin, J. A. Miwa, M. Kondratenko, F. Cicoira, B. G. Sumpter, V. Meunier, D. F. Perepichka, F. Rosei, *Proc. Natl. Acad. Sci. USA* **2010**, *107*, 11200–11204.
[12] J. A. Lipton-Duffin, O. Ivasenko, D. F. Perepichka, F. Rosei, *Small* **2009**, *5*, 592–597.
[13] M. Bieri, M.-T. Nguyen, O. Gröning, J. Cai, M. Treier, K. Aït-Mansour, P. Ruffieux, C. A. Pignedoli, D. Passerone, M. Kastler, K. Müllen, R. Fasel, *J. Am. Chem. Soc.* **2010**, *132*, 16669–16676.
[14] Q. Sun, C. Zhang, Z. Li, H. Kong, Q. Tan, A. Hu, W. Xu, *J. Am. Chem. Soc.* **2013**, *135*, 8448–8451.
[15] L. Grill, M. Dyer, L. Lafferentz, M. Persson, M. V. Peters, S. Hecht, *Nat. Nanotechnol.* **2007**, *2*, 687–691.
[16] Q. Fan, C. Wang, Y. Han, J. Zhu, W. Hieringer, J. Kuttner, G. Hilt, J. M. Gottfried, *Angew. Chem.* **2013**, *125*, 4766–4770; *Angew. Chem. Int. Ed.* **2013**, *52*, 4668–4672.
[17] M. Matena, T. Riehm, M. Stöhr, T. A. Jung, L. H. Gade, *Angew. Chem.* **2008**, *120*, 2448–2451; *Angew. Chem. Int. Ed.* **2008**, *47*, 2414–2417.
[18] S. Weigelt, C. Bombis, C. Busse, M. M. Knudsen, K. V. Gothelf, E. Lægsgaard, F. Besenbacher, T. R. Linderoth, *ACS Nano* **2008**, *2*, 651–660.
[19] S. Weigelt, C. Busse, C. Bombis, M. M. Knudsen, K. V. Gothelf, E. Lægsgaard, F. Besenbacher, T. R. Linderoth, *Angew. Chem.* **2008**, *120*, 4478–4482; *Angew. Chem. Int. Ed.* **2008**, *47*, 4406–4410.
[20] W. Wang, X. Shi, S. Wang, M. Van Hove, N. Lin, *J. Am. Chem. Soc.* **2011**, *133*, 13264–13267.

[21] A. Miura, S. De Feyter, M. M. S. Abdel-Mottaleb, A. Gesquière, P. C. M. Grim, G. Moessner, M. Sieffert, M. Klapper, K. Müllen, F. C. De Schryver, *Langmuir* **2003**, *19*, 6474 – 6482.
[22] R. Tanoue, R. Higuchi, N. Enoki, Y. Miyasato, S. Uemura, N. Kimizuka, A. Z. Stieg, J. K. Gimzewski, M. Kunitake, *ACS Nano* **2011**, *5*, 3923 – 3929.
[23] X.-H. Liu, C.-Z. Guan, S.-Y. Ding, W. Wang, H.-J. Yan, D. Wang, L.-J. Wan, *J. Am. Chem. Soc.* **2013**, *135*, 10470 – 10474.
[24] J. Cai, P. Ruffieux, R. Jaafar, M. Bieri, T. Braun, S. Blankenburg, M. Muoth, A. P. Seitsonen, M. Saleh, X. Feng, K. Müllen, R. Fasel, *Nature* **2010**, *466*, 470 – 473.
[25] L. Lafferentz, V. Eberhardt, C. Dri, C. Africh, G. Comelli, F. Esch, S. Hecht, L. Grill, *Nat. Chem.* **2012**, *4*, 215 – 220.
[26] L. Yin, J. Liebscher, *Chem. Rev.* **2007**, *107*, 133 – 173.
[27] Á. Molnár, *Chem. Rev.* **2011**, *111*, 2251 – 2320.
[28] S. Ditze, M. Stark, M. Drost, F. Buchner, H.-P. Steinrück, H. Marbach, *Angew. Chem.* **2012**, *124*, 11056 – 11059; *Angew. Chem. Int. Ed.* **2012**, *51*, 10898 – 10901.
[29] T. Lin, X. S. Shang, J. Adisoejoso, P. N. Liu, N. Lin, *J. Am. Chem. Soc.* **2013**, *135*, 3576 – 3582.
[30] J. M. Meyers, A. J. Gellman, *Surf. Sci.* **1995**, *337*, 40 – 50.
[31] M. M. Blake, S. U. Nanayakkara, S. A. Claridge, L. C. Fernández-Torres, E. C. H. Sykes, P. S. Weiss, *J. Phys. Chem. A* **2009**, *113*, 13167 – 13172.
[32] M.-T. Nguyen, C. A. Pignedoli, D. Passerone, *Phys. Chem. Chem. Phys.* **2011**, *13*, 154 – 160.
[33] Y. Li, N. Lin, *Phys. Rev. B* **2011**, *84*, 125418.

Received: November 13, 2013
Published online on February 25, 2014